Computers and Chemical Engineering 134 (2020) 106706

Contents lists available at ScienceDirect

Computers and Chemical Engineering

journal homepage: www.elsevier.com/locate/compchemeng

Control Lyapunov-Barrier function-based predictive control of nonlinear processes using machine learning modeling

Zhe Wu [a], Panagiotis D. Christofides [a,b,*]

[a] Department of Chemical and Biomolecular Engineering, University of California, Los Angeles, CA 90095-1592, USA
[b] Department of Electrical and Computer Engineering, University of California, Los Angeles, CA 90095-1592, USA

ARTICLE INFO

Article history:
Received 7 September 2019
Revised 14 December 2019
Accepted 23 December 2019
Available online 26 December 2019

Keywords:
Process safety
Control Lyapunov-Barrier functions
Machine learning
Model predictive control
Nonlinear processes

ABSTRACT

Control Lyapunov-Barrier functions (CLBF) have been adopted to design model predictive controllers (MPC) for input-constrained nonlinear systems to ensure closed-loop stability and process operational safety simultaneously. In this work, a CLBF-MPC using an ensemble of recurrent neural network (RNN) models is proposed with guaranteed closed-loop stability and process operational safety for two types of unsafe regions, i.e., bounded and unbounded sets, for nonlinear processes. The application of the proposed RNN-based CLBF-MPC method is demonstrated through a chemical process example.

1. Introduction

As safety systems and feedback control systems are critical to safe plant operation, they need to act interactively and be integrated to yield cooperative actions to ensure both operational safety and economic performance. Unsafe operations in chemical process industries have resulted in staggering profit losses (Sanders, 2015; Incidents, 2016), which motivate process engineers to coordinate the actions of process safety and control systems from both the ethical perspective of saving lives and property, and also from an economics standpoint for the chemical process industry. To address simultaneously the tasks of stability, safety, and other considerations such as economic optimality, Control Lyapunov functions (CLF) and Control Barrier functions (CBF) have been utilized in designing process control systems. Specifically, process operational safety in the sense that the state is bounded in a safe operating region is guaranteed under the CBFs satisfying Lyapunov-like conditions (Wieland and Allgöwer, 2007; Tee et al., 2009; Niu and Zhao, 2013). CBFs can be naturally unified with CLFs to formulate a quadratic program, which allows for the satisfaction of the objectives of stability and safety (Ames et al., 2014; 2016; Jankovic, 2017). Additionally, Control Lyapunov-Barrier functions have been proposed by combining CBFs and CLFs via weighted average to solve the problem of stabilization of a nonlinear process with guaranteed safety (Romdlony and Jayawardhana, 2016).

To optimize process performance accounting for both closed-loop stability and process operational safety, CLBF-based model predictive control (MPC) has been proposed recently. In Wu et al. (2019a) and Wu and Christofides (2019), the CLBF-based constraints are incorporated in the MPC design to drive the state of an input-constrained nonlinear system to its steady-state while avoiding bounded and unbounded unsafe regions in state-space. In Wu et al. (2018), a new class of economic MPC schemes was developed to achieve simultaneous economic optimality, closed-loop stability and process operational safety by taking advantage of CLBF-based constraints. However, the successful implementation of the above CLBF-based predictive control schemes rely on a hypothesis that an accurate dynamic model for the nonlinear process is available.

Modeling large-scale, complex nonlinear processes has been a major long-standing challenge in process systems engineering. While obtaining a first-principles model that captures nonlinear behavior of a large-scale process is always valuable to address systems-level tasks, data-driven modeling has historically received significant attention (Van Overschee and De Moor, 1994; Viberg, 1995; Billings, 2013; Kosmatopoulos et al., 1995; Trischler and D'Eleuterio, 2016). Designing MPC systems that utilize machine learning modeling techniques to account in real-time for large data sets is a new frontier in control systems as modeling through recurrent neural networks (RNN) has proven to be successful in

* Corresponding author at: Department of Chemical and Biomolecular Engineering, University of California, Los Angeles, CA 90095-1592, USA.
E-mail address: pdc@seas.ucla.edu (P.D. Christofides).

https://doi.org/10.1016/j.compchemeng.2019.106706
0098-1354/

approximating nonlinear dynamical systems (Kosmatopoulos et al., 1995; Trischler and D'Eleuterio, 2016; Ali et al., 2015; Wong et al., 2018). Recent works on machine-learning-based MPC have demonstrated the effectiveness of machine learning tools in the process control field. For example, in Wu et al. (2019b,c), an RNN-based MPC was developed to provide rigorous stability analysis and address practical issues in implementation of machine learning models for a general class of nonlinear systems. This has demonstrated promising potential for use of machine learning techniques in CLBF-based predictive controllers.

Motivated by the above considerations, in this work, we develop a machine-learning-based CLBF-MPC that incorporates an ensemble of RNN models for predicting process dynamics to account for stability and safety considerations in controlling an input-constrained nonlinear process. The rest of the paper is organized as follows: in Section 2, the class of nonlinear systems considered, the stabilizability assumptions, the recurrent neural network models, and the constrained Control Lyapunov-Barrier function are discussed. In Section 3, a CLBF-based model predictive controller using an ensemble of RNN models for predicting future states and optimizing control actions is developed. Sufficient conditions that account for bounded disturbances and a bounded modeling error between the RNN model and the actual nonlinear process are provided to achieve closed-loop stability and safety for the nonlinear process under CLBF-MPC. In Section 4, a chemical process example is utilized to demonstrate the efficacy of the proposed RNN-based CLBF-MPC for both a bounded and an unbounded unsafe region.

2. Preliminaries

2.1. Notation

The Euclidean norm of a vector is denoted by the operator $|\cdot|$ and the weighted Euclidean norm of a vector is denoted by the operator $|\cdot|_Q$ where Q is a positive definite matrix. x^T denotes the transpose of x. $\mathbf{R}_+$ denotes the set $[0, \infty)$. The notation $L_f V(x)$ denotes the standard Lie derivative $L_f V(x) := \frac{\partial V(x)}{\partial x} f(x)$. A scalar continuous function V: $\mathbf{R}^n \to \mathbf{R}$ is proper if the set $\{x \in \mathbf{R}^n \,|\, V(x) \leq k\}$ is compact for all $k \in \mathbf{R}$, or equivalently, V is radially unbounded (Malisoff and Mazenc, 2009). For given positive real numbers β and ϵ, $\mathcal{B}_\beta(\epsilon) := \{x \in \mathbf{R}^n \mid |x - \epsilon| < \beta\}$ is an open ball around ϵ with radius of β. The null set is denoted by $\emptyset$. Set subtraction is denoted by "\", i.e., $A \backslash B := \{x \in \mathbf{R}^n \,|\, x \in A, x \notin B\}$. A function $f(\cdot)$ is of class $\mathcal{C}^1$ if it is continuously differentiable. Given a set $\mathcal{D}$, the boundary and the closure of $\mathcal{D}$ are denoted by $\partial\mathcal{D}$ and $\overline{\mathcal{D}}$, respectively. A continuous function α: $[0, a) \to [0, \infty)$ is said to belong to class $\mathcal{K}$ if it is strictly increasing and is zero only when evaluated at zero.

2.2. Class of systems

The class of continuous-time nonlinear systems considered is described by the following state-space form:

$$\dot{x} = F(x, u, w) := f(x) + g(x)u + h(x)w, \;\; x(t_0) = x_0 \tag{1}$$

where $x \in \mathbf{R}^n$ is the state vector, $u \in \mathbf{R}^m$ is the manipulated input vector, and $w \in \mathbf{W}$ is the disturbance vector, where $\mathbf{W} := \{w \in \mathbf{R}^l \,||w| \leq \theta, \theta \geq 0\}$. The control action constraint is defined by $u \in U := \{u_{\min} \leq u \leq u_{\max}\} \subset \mathbf{R}^m$, where $u_{\min}$ and $u_{\max}$ represent the minimum and the maximum value vectors of inputs allowed, respectively. $f(\cdot)$, $g(\cdot)$, and $h(\cdot)$ are sufficiently smooth vector and matrix functions of dimensions $n \times 1$, $n \times m$, and $n \times l$, respectively. Without loss of generality, the initial time t_0 is taken to be zero ($t_0 = 0$), and it is assumed that $f(0) = 0$, and thus, the origin is a steady-state of the system of Eq. (1) with $w(t) \equiv 0$, (i.e., $(x_s^*, u_s^*) = (0, 0)$, where x_s^* and u_s^* denote the steady-state of Eq. (1)).

2.3. Stabilizability assumptions expressed via lyapunov-based control

We assume that there exists a positive definite and proper Control Lyapunov function (CLF) V for the nominal system of Eq. (1) with $w(t) \equiv 0$ that satisfies the small control property (i.e., for every $\varepsilon > 0$, $\exists\, \delta > 0$, s.t. $\forall\, x \in \mathcal{B}_\delta(0)$, there exists u that satisfies $|u| < \varepsilon$ and $L_f V(x) + L_g V(x) u < 0$, (Sontag, 1989) and the following condition:

$$L_f V(x) < 0, \forall x \in \{z \in \mathbf{R}^n \backslash \{0\} \mid L_g V(z) = 0\} \tag{2}$$

The CLF assumption implies that there exists a stabilizing feedback control law $\Phi(x) \in U$ for the nominal system of Eq. (1) (i.e., $w(t) \equiv 0$) that renders the origin of the closed-loop system asymptotically stable for all x in a neighborhood of the origin in the sense that Eq. (2) holds for $u = \Phi(x) \in U$. An example of a feedback control law can be found in Lin and Sontag (1991). Based on the Lyapunov-based control law $\Phi(x)$, a region ϕ_u where the time-derivative of $V(x)$ is negative under the constrained inputs can be characterized as: $\phi_u = \{x \in \mathbf{R}^n \mid \dot{V} < 0, u = \Phi(x) \in U\}$. Additionally, for any initial state $x_0 \in \Omega_b$, where $\Omega_b := \{x \in \phi_u \,|\, V(x) \leq b, b > 0\}$ is a level set of $V(x)$ inside ϕ_u, it is guaranteed that $x(t)$ for all $t \geq 0$ of the nominal system of Eq. (1) with $w(t) \equiv 0$ under $u = \Phi(x) \in U$ remains in the forward invariant set Ω_b.

2.4. Recurrent neural network

A recurrent neural network (RNN) model that approximates the nonlinear dynamics of the system of Eq. (1) is developed with the following form:

$$\dot{\hat{x}} = F_{nn}(\hat{x}, u) := A\hat{x} + \Theta^T y \tag{3}$$

where $\hat{x} \in \mathbf{R}^n$ is the RNN state vector and $u \in \mathbf{R}^m$ is the manipulated input vector. $y = [y_1, \ldots, y_n, y_{n+1}, \ldots, y_{m+n}] = [\sigma(\hat{x}_1), \ldots, \sigma(\hat{x}_n), u_1, \ldots, u_m] \in \mathbf{R}^{n+m}$ is a vector of both the network state $\hat{x}$ and the input u, where $\sigma(\cdot)$ is the nonlinear activation function (e.g., a sigmoid function $\sigma(x) = 1/(1 + e^{-x})$). A is a diagonal coefficient matrix, i.e., $A = diag\{-a_1, \ldots, -a_n\} \in \mathbf{R}^{n \times n}$, and $\Theta = [\theta_1, \ldots, \theta_n] \in \mathbf{R}^{(m+n) \times n}$ with $\theta_i = b_i[w_{i1}, \ldots, w_{i(m+n)}]$, $i = 1, \ldots, n$. a_i and b_i are constants. w_{ij} is the weight connecting the jth input to the ith neuron where $i = 1, \ldots, n$ and $j = 1, \ldots, (m + n)$. a_i is assumed to be positive such that each state $\hat{x}_i$ is bounded-input bounded-state stable. Throughout the manuscript, we use x to represent the state of the nonlinear system of Eq. (1) and use $\hat{x}$ for the state of the RNN model of Eq. (3).

Additionally, it is noted that the RNN model of Eq. (3) is an input-affine system, and therefore, it can be written in the form that is similar to Eq. (1):

$$\dot{x} = \hat{f}(x) + \hat{g}(x)u \tag{4}$$

where $\hat{f}(\cdot)$ and $\hat{g}(\cdot)$ can be derived from the coefficient matrices A and Θ in Eq. (3) and are assumed to be sufficiently smooth. In the case that the RNN is derived as a discrete model, the approximation of $\hat{f}(\cdot)$ and $\hat{g}(\cdot)$ can be performed via numerical methods that have been discussed in Wu et al. (2019c). Furthermore, to improve generalization performance of an RNN model in terms of better prediction accuracy and applicability in wider operating regime, ensemble learning (Zhang and Ma, 2012; Mendes-Moreira et al., 2012) is used along with neural networks to obtain an ensemble of RNN models such that the final prediction results are calculated by combining multiple RNN models together. The development of an ensemble of RNN models follows a three-step procedure that has been proposed in Wu et al. (2019b): data generation, training process, and ensemble learning. To ensure that the

RNN model of Eq. (3) has the same steady-state as the nonlinear system of Eq. (1), the modeling error is required to be bounded in the training process as follows: $|\nu| = |F(x,u,0) - F_{nn}(x,u)| \leq \gamma|x| \leq \nu_m$, where $\nu_m > 0$ is the upper bound of modeling error ν within the operating region and $\gamma > 0$. Similarly, we assume that there exists a Control Lyapunov function V and a stabilizing controller $u = \Phi_{nn}(x) \in U$ that renders the origin of the RNN system of Eq. (3) asymptotically stable.

2.5. Characterization of unsafe regions

We assume that there is a set $\mathcal{D} \subset \mathbf{R}^n$ within which it is unsafe for the system to be operated, and a safe stability region $\mathcal{U}$ such that $\mathcal{U} \cap \mathcal{D} = \emptyset$ and $\{0\} \subset \mathcal{U}$, within which simultaneous closed-loop stability and process operational safety are achieved in the following sense:

Definition 1. (Wu and Christofides (2019)) Consider the system of Eq. (1) and input constraints $u \in U$. If there exists a control law $u = \Phi(x) \in U$ such that for any initial state $x(t_0) = x_0 \in \mathcal{U}$, $x(t)$ remains inside $\mathcal{U}$, $\forall t \geq 0$, and the origin of the closed-loop system of Eq. (1) can be rendered asymptotically stable, we say that the control law $\Phi(x)$ maintains the process state within a safe stability region $\mathcal{U}$ at all times.

The unsafe region is characterized based on the safety analysis of processes either from first-principles models or process operational data. Specifically, according to Wu and Christofides (2019), there are two types of unsafe regions: 1) bounded sets, which are generally encountered in motion planning for robots and self-driving cars, and 2) unbounded sets, which are very common in chemical processes, for example, an unsafe region within which the temperature in a reactor is above a threshold that indicates an unsafe operation. In this work, both bounded unsafe region (denoted by $\mathcal{D}_b$) and unbounded unsafe region (denoted by $\mathcal{D}_u$) will be discussed. A CLBF-based predictive controller based on machine learning models will be developed to ensure that the closed-loop state can be driven to the steady-state and avoid the unsafe region (bounded and unbounded).

2.6. Stabilization and safety via control lyapunov-Barrier function-based control

In Romdlony and Jayawardhana (2016), the Control Lyapunov-Barrier function is formulated via the weighted average of a Control Lyapunov function and a Control Barrier function (CBF). Specifically, given a CLF that satisfies Eq. (2) and the small control property, closed-loop stability is achieved under the controller $u = \Phi_{nn}(x) \in U$ for the RNN system of Eq. (3). Additionally, CBF is proposed in Wieland and Allgöwer (2007) to ensure process operational safety. The definition of a CBF can be found in Romdlony and Jayawardhana (2016) and Wu et al. (2019a). Based on CBFs and CLFs, a constrained CLBF was proposed in Wu and Christofides (2019) and Wu et al. (2019a) to ensure process safety and stability accounting for input constraints. The definition of a constrained CLBF is as follows:

Definition 2. Given a set of unsafe points in state-space $\mathcal{D}$, a proper, lower-bounded and $\mathcal{C}^1$ function $W_c(x)$: $\mathbf{R}^n \to \mathbf{R}$ is a constrained CLBF if $W_c(x)$ has a minimum at the origin and also satisfies the following properties:

$$W_c(x) > \rho, \quad \forall\, x \in \mathcal{D} \subset \phi_{uc} \tag{5a}$$

$$L_{\hat{f}} W_c(x) < 0,$$
$$\forall\, x \in \{z \in \phi_{uc} \backslash (\mathcal{D} \cup \{0\} \cup \mathcal{X}_e) \mid L_{\hat{g}} W_c(z) = 0\} \tag{5b}$$

$$\mathcal{U}_\rho := \{x \in \phi_{uc} \mid W_c(x) \leq \rho\} \neq \emptyset \tag{5c}$$

where $\rho \in \mathbf{R}$, and $\mathcal{X}_e := \{x \in \phi_{uc} \backslash (\mathcal{D} \cup \{0\}) \mid \partial W_c(x)/\partial x = 0\}$ is a set of states for the RNN model of Eq. (4) where $L_{\hat{f}} W_c(x) = 0$ (for $x \neq 0$) due to $\partial W_c(x)/\partial x = 0$. $\hat{f}$ and $\hat{g}$ are from the RNN model in the form of Eq. (4). A feedback control law $u = \Phi_{nn}(x) \in U$ that renders the origin exponentially stable within an open neighborhood ϕ_{uc} that includes the origin in its interior is assumed to exist for the RNN system of Eq. (3) (also in the form of Eq. (4)) in the sense that there exists a $\mathcal{C}^1$ constrained Control Lyapunov-Barrier function $W_c(x)$ that has a minimum at the origin and satisfies the following inequalities $\forall x \in \phi_{uc}$:

$$\hat{c}_1|x|^2 \leq W_c(x) - \rho_0 \leq \hat{c}_2|x|^2, \tag{6a}$$

$$\frac{\partial W_c(x)}{\partial x} F_{nn}(x, \Phi_{nn}(x)) \leq -\hat{c}_3|x|^2, \forall x \in \phi_{uc} \backslash \mathcal{B}_\delta(x_e) \tag{6b}$$

$$\left| \frac{\partial W_c(x)}{\partial x} \right| \leq \hat{c}_4|x| \tag{6c}$$

where $\hat{c}_j$, $j = 1,\ 2,\ 3,\ 4$ are positive real numbers, $W_c(0) = \rho_0$ is the global minimum value of $W_c(x)$ in ϕ_{uc}, and $\mathcal{B}_\delta(x_e)$ is a small neighborhood around $x_e \in \mathcal{X}_e$. $F_{nn}(x,\ u)$ is the RNN system of Eq. (3). It is noted that Eq. (6b) does not hold for $x \in \mathcal{B}_\delta(x_e)$ since $\frac{\partial W_c(x)}{\partial x}$ is close to zero in a neighborhood around the stationary point x_e, where $\frac{\partial W_c(x)}{\partial x} = 0$. Additionally, by continuity and the smoothness assumed for f, g and h in the nonlinear system of Eq. (1), there exist positive constants M, L_x, L_w, L_x', L_w' such that the following inequalities hold for all $x, x' \in \mathcal{U}_\rho, u \in U$, and $w \in W$:

$$|F(x,u,w)| \leq M \tag{7a}$$

$$|F(x,u,w) - F(x',u,0)| \leq L_x|x - x'| + L_w|w| \tag{7b}$$

$$\left| \frac{\partial W_c(x)}{\partial x} F(x,u,w) - \frac{\partial W_c(x')}{\partial x} F(x',u,0) \right| \leq L_x'|x - x'| + | \leq L_w'|w_m| \tag{7c}$$

An example of the stabilizing control law $\Phi_{nn}(x)$ associated with CLBFs can be found in Wu et al. (2018) and Wu and Christofides (2019); Wu et al. (2019a), in which a Lyapunov-based control law with the form of the universal Sontag controller (Lin and Sontag, 1991) is used with $W_c(x)$ replacing the Lyapunov function $V(x)$. It should be noted that the CLBF of Eq. (5) and the set ϕ_{uc} are designed based on the RNN model of Eq. (3) (also in the form of Eq. (4), i.e., $\dot{x} = \hat{f}(x) + \hat{g}(x)u$) since the nonlinear system of Eq. (1) is assumed to be unknown. A constrained CLBF that satisfies all the conditions in Eq. (5) can be developed by first designing a CLF and a CBF separately, and then combining them together via the construction method in Romdlony and Jayawardhana (2016) and Wu et al. (2019a) Additionally, it is noted that the construction method in Wu et al. (2019a) is not restricted to a two-dimensional system, and therefore, can be applied to the design of CLBFs for large-scale systems.

Consider the RNN model of Eq. (3) (also in the form of Eq. (4)) with a constrained CLBF $W_c(x)$ of Eq. (5). Simultaneous closed-loop stability and safety can be derived for both a bounded unsafe region $\mathcal{D}_b$ and an unbounded unsafe region $\mathcal{D}_u$ following the similar analysis that has been performed for the nominal system of Eq. (1) in Wu and Christofides (2019) (see Theorem 1 and 2 in Wu and Christofides (2019)). Specifically, it is noted that in the case of a bounded unsafe set, there exist stationary points (other than the origin) in state-space (i.e., $\mathcal{X}_e$ in Eq. (5b)), and thus, a

continuous controller cannot render the origin exponentially stable Braun and Kellett (2018). This issue can be addressed by designing the stationary points to be saddle points and then implementing discontinuous control actions at saddle points to drive the state away from them in the direction of decreasing $W_c(x)$ ((Wu and Christofides, 2019; Wu et al., 2019a)). However, in the presence of an unbounded unsafe region, the origin is the unique stationary point in state-space, thereby closed-loop stability and process operational safety can be readily derived under the controller $u = \Phi_{nn}(x) \in U$. The following theorem provides sufficient conditions under which closed-loop stability and process operational safety are achieved simultaneously for the RNN system of Eq. (3) under the control law designed based on a constrained CLBF of Eq. (5).

Theorem 1. *Consider that a constrained CLBF $W_c(x)$: $\mathbf{R}^n \rightarrow \mathbf{R}$ that has a minimum at the origin and meets the conditions of Eq. (5), exists for the RNN system of Eq. (3). The controller $u = \Phi_{nn}(x) \in U$ that satisfies Eq. (6) guarantees that the closed-loop state stays in $\mathcal{U}_\rho$ for all times for any $x_0 \in \mathcal{U}_\rho$. Additionally, the origin can be rendered exponentially stable under $u = \Phi_{nn}(x) \in U$, for all $x_0 \in \mathcal{U}_\rho$ in the presence of an unbounded unsafe region $\mathcal{D}_u$; however, discontinuous control actions $u = \bar{u}(x) \in U$ that decrease $W_c(x)$ are required at saddle points x_e to ensure exponential stability of the origin in the presence of a bounded unsafe region $\mathcal{D}_b$ in state-space.*

Proof. To demonstrate that the state is bounded in the safe operating region $\mathcal{U}_\rho$ for all times, we need to show that there exists a controller $u = \Phi_{nn}(x) \in U$ such that $\dot{W}_c \leq 0$ holds for all $x \in \mathcal{U}_\rho$. This has been proven in Wu et al. (2018, 2019a) by showing that the universal Sontag controller (Lin and Sontag, 1991) with $W_c(x)$ replacing the Lyapunov function $V(x)$ can be utilized as $\Phi_{nn}(x)$. Additionally, since $\mathcal{U}_\rho$ is characterized as a level set of $W_c(x)$ in ϕ_{uc} within which Eq. (6) is satisfied, we can further demonstrate that the origin can be rendered exponentially stable under $u = \Phi_{nn}(x) \in U$. The issue of saddle points in the presence of a bounded unsafe region is handled by discontinuous control actions $\bar{u}(x)$ (i.e., $\bar{u}(x) \neq \Phi_{nn}(x)$). The detailed proofs for both bounded and unbounded unsafe regions follow closely to those for Theorem 1 and 2 in Wu and Christofides (2019), and is omitted here. □

Remark 1. As we assume that the nonlinear system of Eq. (1) is unknown, the CLBF of Eq. (5) and the safe operating region $\mathcal{U}_\rho$ are characterized based on the RNN system of Eq. (3). Theorem 1 is established to demonstrate that closed-loop stability and operational safety are achieved for the RNN system of Eq. (3) via a stabilizing controller $u = \Phi_{nn}(x) \in U$ that is defined with respect to the CLBF of Eq. (5). In the following section, we will demonstrate that the CLBF-based controller $u = \Phi_{nn}(x) \in U$ also guarantees simultaneous closed-loop stability and operational safety for the nonlinear system of Eq. (1) provided that the modeling error between the nonlinear system of Eq. (1) and the RNN system of Eq. (3) is sufficiently small.

3. CLBF-Based MPC using an ensemble of RNN models

This section presents the formulation of the CLBF-based MPC (CLBF-MPC) that incorporates an ensemble of RNN models for predicting future states. We first demonstrate that the stability and safety properties in Theorem 1 hold for the nominal system of Eq. (1) (i.e., $w(t) \equiv 0$) under the CLBF-based controller $u = \Phi_{nn}(x) \in U$ that is designed to stabilize the RNN system of Eq. (3) with guaranteed safety. Subsequently, the CLBF-MPC is developed to drive the state to a small neighborhood around the origin while optimizing process performance under sample-and-hold implementation of control actions. To proceed, the following proposition is first developed to obtain an upper bound for the error between the states predicted by the RNN model of Eq. (3) and the states of the nonlinear process of Eq. (1) in the presence of bounded disturbances (i.e., $|w(t)| \leq w_m$) and a bounded modeling error (i.e., $|\nu| = |F(x,u,0) - F_{nn}(x,u)| \leq \gamma|x| \leq \nu_m$).

Proposition 1. *Consider the nonlinear system $\dot{x} = F(x,u,w)$ of Eq. (1) in the presence of bounded disturbances $|w(t)| \leq w_m$. Assuming that the RNN model $\dot{\hat{x}} = F_{nn}(\hat{x},u)$ of Eq. (3) has the same initial condition $x_0 = \hat{x}_0 \in \mathcal{U}_\rho$ as the nonlinear system of Eq. (1), there exists a class $\mathcal{K}$ function $f_w(\cdot)$ and a positive constant κ such that the following inequalities hold $\forall x, \hat{x} \in \mathcal{U}_\rho$ and $w(t) \in W$:*

$$|x(t) - \hat{x}(t)| \leq f_w(t) := \frac{L_w w_m + \nu_m}{L_x}(e^{L_x t} - 1) \tag{8a}$$

$$W_c(x) \leq W_c(\hat{x}) + \frac{\hat{c}_4\sqrt{\rho - \rho_0}}{\sqrt{\hat{c}_1}}|x - \hat{x}| + \kappa|x - \hat{x}|^2 \tag{8b}$$

Proof. Let $e(t) = x(t) - \hat{x}(t)$ denote the error vector between the solutions of the system $\dot{x} = F(x,u,w)$ and the RNN model $\dot{\hat{x}} = F_{nn}(\hat{x},u)$. The time-derivative of $e(t)$ is obtained as follows:

$$\begin{aligned} |\dot{e}| &= |F(x,u,w) - F_{nn}(\hat{x},u)| \\ &\leq |F(x,u,w) - F(\hat{x},u,0)| + |F(\hat{x},u,0) - F_{nn}(\hat{x},u)| \end{aligned} \tag{9}$$

Using Eq. (7b), the upper bound for the first term of Eq. (9) is derived by the following inequality for all $x, \hat{x} \in \mathcal{U}_\rho$ and $w(t) \in W$:

$$\begin{aligned} |F(x,u,w) - F(\hat{x},u,0)| &\leq L_x|x(t) - \hat{x}(t)| + L_w|w(t)| \\ &\leq L_x|x(t) - \hat{x}(t)| + L_w w_m \end{aligned} \tag{10}$$

Additionally, it is noticed that the second term of Eq. (9) represents the modeling error (i.e., $|\nu| = |F(\hat{x},u,0) - F_{nn}(\hat{x},u)|$), and is bounded by $|\nu| \leq \nu_m$. Therefore, the upper bound for $\dot{e}(t)$ in Eq. (9) is obtained as follows:

$$\begin{aligned} |\dot{e}(t)| &\leq L_x|x(t) - \hat{x}(t)| + L_w w_m + \nu_m \\ &\leq L_x|e(t)| + L_w w_m + \nu_m \end{aligned} \tag{11}$$

Given the zero initial condition (i.e., $e(0) = 0$), the upper bound for $|e(t)|$ is derived for all $x(t), \hat{x}(t) \in \mathcal{U}_\rho$ and $|w(t)| \leq w_m$ as follows:

$$|e(t)| = |x(t) - \hat{x}(t)| \leq f_w(t) \tag{12}$$

where

$$f_w(t) := \frac{L_w w_m + \nu_m}{L_x}(e^{L_x t} - 1)$$

Moreover, since $W_c(x)$ is continuous and bounded on compact sets, the following inequality is derived based on the Taylor series expansion of $W_c(x)$ around $\hat{x}$, $\forall x, \hat{x} \in \mathcal{U}_\rho$:

$$W_c(x) \leq W_c(\hat{x}) + \frac{\partial W_c(\hat{x})}{\partial x}|x - \hat{x}| + \kappa|x - \hat{x}|^2 \tag{13}$$

where κ is a positive real number and the term $\kappa|x - \hat{x}|^2$ is used to bound the high order terms of the Taylor series of $W_c(x)$, $\forall x, \hat{x} \in \mathcal{U}_\rho$. The following inequality is derived using Eqs. (6a), (6c) and (12):

$$\begin{aligned} W_c(x) &\leq W_c(\hat{x}) + \frac{\hat{c}_4\sqrt{\rho - \rho_0}}{\sqrt{\hat{c}_1}}|x - \hat{x}| + \kappa|x - \hat{x}|^2 \\ &\leq W_c(\hat{x}) + \frac{\hat{c}_4\sqrt{\rho - \rho_0}}{\sqrt{\hat{c}_1}}f_w(t) + \kappa f_w(t)^2 \end{aligned} \tag{14}$$

This completes the proof of Proposition 1. □

3.1. CLBF-based control using RNN models

The following propositions are developed to demonstrate that the controller $u = \Phi_{nn}(x) \in U$ designed for the RNN model of

Eq. (3) is able to maintain the state of the nominal system of Eq. (1) within the safe operating region $\mathcal{U}_\rho$ provided that the modeling error is sufficiently small. We first consider the case of an unbounded unsafe region, for which exponential stability is achieved for the closed-loop nominal system of Eq. (1) under $u = \Phi_{nn}(x) \in U$.

Proposition 2. *Consider the nominal system of Eq. (1) (i.e., $w(t) \equiv 0$) with an unbounded unsafe region $\mathcal{D}_u$ under the feedback controller $u = \Phi_{nn}(x) \in U$ that satisfies Eq. (6) for all $x \in \mathcal{U}_\rho$. If there exists a positive real number $\gamma < \hat{c}_3/\hat{c}_4$ such that for all $x \in \mathcal{U}_\rho$ and $u \in U$, the modeling error between the RNN model of Eq. (3) and the nonlinear system of Eq. (1) is constrained by $|\nu| = |F(x,u,0) - F_{nn}(x,u)| \leq \gamma|x|$, then the stability and safety properties in Theorem 1 also hold for the nominal closed-loop system of Eq. (1) under $u = \Phi_{nn}(x) \in U$.*

Proof. To demonstrate that the origin of the nominal system of Eq. (1) (i.e., $w(t) \equiv 0$) can be rendered exponentially stable under $u = \Phi_{nn}(x) \in U$, we prove that there exists a positive real number $\tilde{c}_3$ such that $\frac{\partial W_c(x)}{\partial x} F(x, \Phi_{nn}(x), 0) \leq -\tilde{c}_3|x|^2$, $\forall x \in \mathcal{U}_\rho$ holds. It is noted that in the presence of an unbounded unsafe region, there is no saddle point within the safe operation region $\mathcal{U}_\rho$, and therefore, Eq. (6) holds for all $x \in \mathcal{U}_\rho$. The time-derivative of W_c is derived as follows using Eqs. (6b) and (6c):

$$\begin{aligned}\dot{W}_c &= \frac{\partial W_c(x)}{\partial x} F(x, \Phi_{nn}(x), 0) \\ &= \frac{\partial W_c(x)}{\partial x} (F_{nn}(x, \Phi_{nn}(x)) + F(x, \Phi_{nn}(x), 0) - F_{nn}(x, \Phi_{nn}(x))) \\ &\leq -\hat{c}_3|x|^2 + \hat{c}_4|x|(F(x, \Phi_{nn}(x), 0) - F_{nn}(x, \Phi_{nn}(x))) \\ &\leq -\hat{c}_3|x|^2 + \hat{c}_4\gamma|x|^2 \end{aligned} \tag{15}$$

Let $\tilde{c}_3 = -\hat{c}_3 + \hat{c}_4\gamma$. It is obtained that $\dot{W}_c \leq -\tilde{c}_3|x|^2 \leq 0$ if γ is chosen to satisfy $\gamma < \hat{c}_3/\hat{c}_4$. Therefore, following the proof of closed-loop stability and safety for the RNN system of Eq. (3) in Theorem 1, the controller $u = \Phi_{nn}(x) \in U$ can drive the state of the nominal system of Eq. (1) to the origin while avoiding the unbounded unsafe region $\mathcal{D}_u$ for all times. This completes the proof of simultaneous closed-loop stability and operational safety for any initial condition x_0 in the safe operating region $\mathcal{U}_\rho$ of Eq. (5c). □

The following proposition is developed to provide sufficient conditions under which simultaneous closed-loop stability and process operational safety are guaranteed for the nominal system of Eq. (1) with a bounded unsafe region $\mathcal{U}_b$ accounting for the existence of saddle points x_e in the safe operating region $\mathcal{U}_\rho$.

Proposition 3. *Consider the nominal system of Eq. (1) with a bounded unsafe region $\mathcal{D}_b$ under the controller $u = \Phi_{nn}(x) \in U$ that satisfies Eq. (6) for all $x \in \mathcal{U}_\rho$. If there exists a positive real number $\gamma < \hat{c}_3/\hat{c}_4$ such that for all $x \in \mathcal{U}_\rho$ and $u \in U$, the modeling error is constrained by $|\nu| = |F(x,u,0) - F_{nn}(x,u)| \leq \gamma|x|$, and Eq. (16) is satisfied under discontinuous control actions $u = \bar{u}(x) \in U$ when $x(t_k) = \hat{x}(t_k) \in \mathcal{B}_\delta(x_e)$,*

$$W_c(\hat{x}(t)) < W_c(\hat{x}(t_k)) - f_e(t - t_k), \quad \forall t > t_k \tag{16}$$

where

$$f_e(t - t_k) := \frac{\hat{c}_4\sqrt{\rho - \rho_0}}{\sqrt{\hat{c}_1}} f_w(t - t_k) - \kappa f_w(t - t_k)^2$$

and $f_w(t)$ is given in Eq. (12), then the stability and safety properties in Theorem 1 also hold for the nominal closed-loop system of Eq. (1) with a bounded unsafe region $\mathcal{D}_b$ under $u = \Phi_{nn}(x) \in U$ and $u = \bar{u}(x) \in U$.

Proof. Since there exist saddle points x_e in the safe operating region $\mathcal{U}_\rho$ in the presence of a bounded unsafe region, the origin of the nominal system of Eq. (1) (i.e., $w(t) \equiv 0$) cannot be rendered exponentially stable under the continuous controller $u = \Phi_{nn}(x) \in U$. To address the issue of saddle points x_e, another set of control actions $\bar{u}$ will be applied within a neighborhood around x_e to drive the state away from saddle points and towards the origin. Specifically, in the presence of a bounded unsafe region, it is readily shown that Eq. (15) still holds for all $x \in \mathcal{U}_\rho \backslash \mathcal{B}_\delta(x_e)$ since Eq. (6b) is satisfied in $\mathcal{U}_\rho \backslash \mathcal{B}_\delta(x_e)$. This implies that in the presence of a bounded unsafe region, the controller $u = \Phi_{nn}(x) \in U$ that is designed to achieve closed-loop stability and safety for the RNN model of Eq. (3) is also able to maintain the state of the closed-loop system of Eq. (1) within $\mathcal{U}_\rho$ for all times.

Subsequently, we prove that the discontinuous control actions $u = \bar{u}(x) \in U$ that are designed for the RNN model of Eq. (3) around saddle points can drive the state of the nonlinear system of Eq. (1) away from saddle points in the direction of decreasing $W_c(x)$. Proposition 1 has established that starting from the same initial condition, the error between the states of the RNN system of Eq. (3) and of the nonlinear system of Eq. (1) is bounded under the same control actions, and therefore, the evolution of $W_c(x)$ based on the state of the nominal system of Eq. (1) is also bounded by Eq. (14) accounting for the modeling error and bounded disturbances. Assuming that the state enters a neighborhood around the saddle points at $t = t_k$ (i.e., $\hat{x}(t_k) = x(t_k) \in \mathcal{B}_\delta(x_e)$), if the discontinuous control actions $\bar{u}(\hat{x})$ that are determined for the RNN model of Eq. (3) satisfy Eq. (16) for all $x \in \mathcal{B}_\delta(x_e)$, the following inequality can be derived from Eqs. (14) and (16) to show that the value of $W_c(x)$ based on the state of the nonlinear system of Eq. (1) is guaranteed to decrease $\forall t > t_k$:

$$\begin{aligned} W_c(x(t)) &\leq W_c(\hat{x}(t)) + \frac{\hat{c}_4\sqrt{\rho - \rho_0}}{\sqrt{\hat{c}_1}} f_w(t - t_k) + \kappa f_w(t - t_k)^2, \\ &< W_c(\hat{x}(t_k)) \end{aligned} \tag{17}$$

Therefore, the state of the nonlinear system of Eq. (1) can escape from saddle points under the discontinuous control actions $u = \bar{u}(x) \in U$ that are designed for the RNN system of Eq. (3) provided that the decreasing rate of $W_c(x)$ of Eq. (16) is satisfied. This implies that for any initial condition $x_0 \in \mathcal{U}_\rho$, the closed-loop state of the nonlinear system of Eq. (1) can be driven to the origin while avoiding the bounded unsafe region $\mathcal{D}_b$ under the controllers $u = \Phi_{nn}(x) \in U$ and $u = \bar{u}(x) \in U$. □

Remark 2. From Propositions 2 and 3, it is demonstrated that the controller $u = \Phi_{nn}(x) \in U$ that is designed to stabilize the RNN system of Eq. (3) (i.e., $\dot{\hat{x}} = F_{nn}(\hat{x}, u)$) guarantees simultaneous closed-loop stability and operational safety for the nominal system of Eq. (1) (i.e., $w(t) \equiv 0$). Specifically, in the case of an unbounded unsafe region, the state of the nominal system of Eq. (1) is bounded in the safe operating region $\mathcal{U}_\rho$ for all times and the origin can be rendered exponentially stable under $u = \Phi_{nn}(x) \in U$. However, to ensure closed-loop stability and operational safety for the nominal system of Eq. (1) in the presence of a bounded unsafe region, in addition to the controller $u = \Phi_{nn}(x) \in U$ that is applied everywhere except the neighborhood around saddle points (i.e., $\mathcal{B}_\delta(x_e)$), a set of discontinuous control actions $u = \bar{u}(x) \in U$ that satisfy Eq. (16) is required for the state in $\mathcal{B}_\delta(x_e)$.

3.2. Sample-and-hold implementation of CLBF-based controller

In this section, we present the stability properties of the CLBF-based controllers $u = \Phi_{nn}(x) \in U$ and $u = \bar{u}(x) \in U$ (for a bounded unsafe region) for the nonlinear system of Eq. (1) accounting for bounded disturbances (i.e., $|w(t)| \leq w_m$) and sample-and-hold implementation of the control actions. To proceed, we need the following proposition to demonstrate that under the controllers $u = \Phi_{nn}(x) \in U$ and $u = \bar{u}(x) \in U$ implemented in a sample-and-hold fashion, i.e., $u(t) = u(t_k)$, $\forall t \in [t_k, t_{k+1})$, where $t_{k+1} := t_k + \Delta$ and

Δ is the sampling period, the closed-loop state $x(t)$ of the nonlinear system of Eq. (1) is bounded in $\mathcal{U}_\rho$ for all times, and will be ultimately driven to a small neighborhood $\mathcal{U}_{\rho_{\min}}$ around the origin.

Proposition 4. *Consider the system of Eq. (1) under the sample-and-hold implementation of the controller $u = \Phi_{nn}(x) \in U$ that meets the conditions of Eq. (6). If Eq. (16) is satisfied under the controller $u = \bar{u}(x) \in U$ in a sample-and-hold fashion for $x \in \mathcal{B}_\delta(x_e)$, and there exist $\epsilon_w > 0$, $\Delta > 0$ and $\rho > \rho_{\min} > \rho_{nn} > \rho_s$ that satisfy*

$$-\frac{\tilde{c}_3}{\hat{c}_2}(\rho_s - \rho_0) + L_x' M\Delta + L_w' w_m \leq -\epsilon_w \tag{18}$$

and

$$\rho_{nn} := \max\{W_c(\hat{x}(t+\Delta)) \mid \hat{x}(t) \in \mathcal{U}_{\rho_s}, u \in U\} \tag{19a}$$

$$\rho_{min} \geq \rho_{nn} + f_e(\Delta) \tag{19b}$$

where $f_e(t)$ is given by Eq. 16, then for any $x(t_k) \in \mathcal{U}_\rho \backslash \mathcal{U}_{\rho_s}$, $W_c(x(t))$ based on the state of the nonlinear system of Eq. (1) is guaranteed to decrease within every sampling period, and thus, can be bounded in $\mathcal{U}_\rho$ for all times and ultimately bounded in $\mathcal{U}_{\rho_{\min}}$.

Proof. Assuming $x(t_k) = \hat{x}(t_k) \in \mathcal{U}_\rho \backslash \mathcal{U}_{\rho_s}$, the time-derivative of $W_c(x)$ for the nonlinear system of Eq. (1) in the presence of bounded disturbances (i.e., $|w| \leq w_m$) is derived as follows:

$$\begin{aligned}\dot{W}_c(x(t)) &= \frac{\partial W_c(x(t))}{\partial x} F(x(t), \Phi_{nn}(x(t_k)), w) \\ &= \frac{\partial W_c(x(t_k))}{\partial x} F(x(t_k), \Phi_{nn}(x(t_k)), 0) \\ &\quad + \frac{\partial W_c(x(t))}{\partial x} F(x(t), \Phi_{nn}(x(t_k)), w) \\ &\quad - \frac{\partial W_c(x(t_k))}{\partial x} F(x(t_k), \Phi_{nn}(x(t_k)), 0)\end{aligned} \tag{20}$$

Based on Eqs. (6b) and (15) and the Lipschitz condition in Eq. (7), the following inequality is obtained for $\dot{W}_c(x(t))$ for all $t \in [t_k, t_{k+1})$ and $x(t_k) \in \mathcal{U}_\rho \backslash (\mathcal{U}_{\rho_s} \cup \mathcal{B}_\delta(x_e))$:

$$\begin{aligned}\dot{W}_c(x(t)) &\leq -\frac{\tilde{c}_3}{\hat{c}_2}(\rho_s - \rho_0) + \frac{\partial W_c(x(t))}{\partial x} F(x(t), \Phi_{nn}(x(t_k)), w) \\ &\quad - \frac{\partial W_c(x(t_k))}{\partial x} F(x(t_k), \Phi_{nn}(x(t_k)), 0) \\ &\leq -\frac{\tilde{c}_3}{\hat{c}_2}(\rho_s - \rho_0) + L_x' |x(t) - x(t_k)| + L_w' |w| \\ &\leq -\frac{\tilde{c}_3}{\hat{c}_2}(\rho_s - \rho_0) + L_x' M\Delta + L_w' w_m\end{aligned} \tag{21}$$

It is noted that Eq. (21) does not hold for $x \in \mathcal{B}_\delta(x_e)$ since Eqs. (6b) and (15) may not hold in the neighborhood around saddle points where $\frac{\partial W_c(x)}{\partial x}$ is close to zero. If Eq. (18) is satisfied, we can obtain the following inequality based on Eq. (21) for all $x(t_k) \in \mathcal{U}_\rho \backslash \mathcal{U}_{\rho_s}$ and $t \in [t_k, t_{k+1})$:

$$\dot{W}_c(x(t)) \leq \quad -\epsilon_w \tag{22}$$

From Eq. (22), the boundedness of the state of the closed-loop system of Eq. (1) in the safe operating region $\mathcal{U}_\rho$ is obtained under the sample-and-hold implementation of $u = \Phi_{nn}(x) \in U$ for any initial condition $x_0 \in \mathcal{U}_\rho$.

Additionally, to ensure that the state of the nonlinear system of Eq. (1) moves towards the origin and ultimately enters a small neighborhood $\mathcal{U}_{\rho_s}$ around the origin instead of converging to saddle points, the controller $u = \bar{u}(x(t_{k+i})) \in U$, $\forall t \in [t_{k+i}, t_{k+i+1})$, $i = 0, 1, 2, \ldots$ is applied to drive the state away from saddle points when $x(t_k) = \hat{x}(t_k) \in \mathcal{B}_\delta(x_e)$. If Eq. (16) is satisfied under the sample-and-hold implementation of $u = \bar{u}(\hat{x}) \in U$, it is demonstrated from Eq. (17) in Proposition 3 that $W_c(x(t)) < W_c(x(t_k))$ holds for the nonlinear system of Eq. (1), $\forall t > t_k$. Therefore, $W_c(x)$ will keep decreasing until the state of the nonlinear system of Eq. (1) leaves the neighborhood around saddle points. After that, the controller $u = \Phi_{nn}(x) \in U$ will be applied again to drive the state towards the origin.

It remains to show that once the state enters $\mathcal{U}_{\rho_s}$ (i.e., $x(t_k) = \hat{x}(t_k) \in \mathcal{U}_{\rho_s}$), it is bounded in $\mathcal{U}_{\rho_{\min}}$ for the remaining time $t \geq t_k$. According to the definition of $\mathcal{U}_{\rho_{nn}}$ in Eq. (19a), it is shown that $\mathcal{U}_{\rho_{nn}}$ is the largest level set of $W_c(\hat{x})$ that the state of the RNN system of Eq. (3) can reach within one sampling period if starting from $\mathcal{U}_{\rho_s}$. Additionally, $\mathcal{U}_{\rho_{\min}}$ of Eq. (19b) is the corresponding largest level set of $W_c(x)$ based on the state of the nonlinear system of Eq. (1) when the RNN state $\hat{x}$ is bounded in $\mathcal{U}_{\rho_{nn}}$.

Since $\dot{W}_c \leq -\epsilon_w$ may not hold for the state in $\mathcal{U}_{\rho_s}$ under the sample-and-hold implementation of $u = \Phi_{nn}(x) \in U$, the sets $\mathcal{U}_{\rho_{nn}}$ and $\mathcal{U}_{\rho_{\min}}$ are characterized to guarantee that the states of the RNN system of Eq. (3) and of the nonlinear system of Eq. (1) are bounded in the neighborhoods around the origin that are slightly larger than $\mathcal{U}_{\rho_s}$. Additionally, $\mathcal{U}_{\rho_{nn}}$ can be characterized from extensive open-loop simulations for all $u \in U$ and $x \in \mathcal{U}_{\rho_s}$. Subsequently, $\mathcal{U}_{\rho_{\min}}$ of Eq. (19b) is characterized based on $\mathcal{U}_{\rho_{nn}}$ to account for the impact of modeling error and bounded disturbances within one sampling period.

This completes the proof of Proposition 4 by showing that the state of the nonlinear system of Eq. (1) with bounded disturbances (i.e., $|w(t)| \leq w_m$) can be maintained in the safe operating region $\mathcal{U}_\rho$ for all times, and ultimately be bounded in $\mathcal{U}_{\rho_{\min}}$ under the sample-and-hold implementation of $u = \Phi_{nn}(x) \in U$ and $u = \bar{u}(x) \in U$. □

3.3. Formulation of CLBF-MPC

The CLBF-MPC design is represented by the following optimization problem:

$$\mathcal{J} = \min_{u \in S(\Delta)} \int_{t_k}^{t_{k+N}} L(\tilde{x}(t), u(t)) dt \tag{23a}$$

$$\text{s.t.} \quad \dot{\tilde{x}}(t) = \frac{1}{N_e} \sum_{j=1}^{N_e} F_{nn}^j(\tilde{x}(t), u(t)) \tag{23b}$$

$$\tilde{x}(t_k) = x(t_k) \tag{23c}$$

$$u(t) \in U, \ \forall \ t \in [t_k, t_{k+N}) \tag{23d}$$

$$\begin{aligned}&\dot{W}_c(x(t_k), u(t_k)) \leq \dot{W}_c(x(t_k), \Phi_{nn}(t_k)) \\ &\text{if } W_c(x(t_k)) > \rho_{nn} \text{ and } x(t_k) \notin \mathcal{B}_\delta(x_e)\end{aligned} \tag{23e}$$

$$\begin{aligned}&W_c(\tilde{x}(t)) \leq \rho_{nn}, \ \forall \ t \in [t_k, t_{k+N}), \\ &\text{if } W_c(x(t_k)) \leq \rho_{nn}\end{aligned} \tag{23f}$$

$$\begin{aligned}&W_c(\tilde{x}(t)) < W_c(x(t_k)) - f_e(t - t_k), \ \forall \ t \in (t_k, t_{k+N}), \\ &\text{if } x(t_k) \in \mathcal{B}_\delta(x_e)\end{aligned} \tag{23g}$$

where $\tilde{x}(t)$ is the predicted state trajectory, $S(\Delta)$ is the set of piecewise constant functions with period Δ, and N is the number of sampling periods in the prediction horizon. The cost function $L(\tilde{x}(t), u(t))$ is generally in a quadratic form that has the minimum value at the equilibrium of the system of Eq. (1) : $|\tilde{x}(t)|_{Q_L}^2 + |u(t)|_{R_L}^2$, where Q_L and R_L are positive definite matrices. The predicted states $\tilde{x}(t)$, $t \in [t_k, t_{k+N})$ are calculated by taking the average of an ensemble of RNN models F_{nn}^j, $j = 1, \ldots, N_e$ in Eq. (23b),

where N_e is the number of RNN models in the ensemble. The objective function of Eq. (23a) is the time integral of $L(\tilde{x}(t), u(t))$ over the prediction horizon. The input constraints of Eq. (23d) are applied over the entire prediction horizon. The state measurement of Eq. (23c) at $t = t_k$ is taken as the initial condition for the RNN models of Eq. (23b). The constraints of Eqs. (23e)–(23g) in the CLBF-MPC optimization problem are utilized to ensure closed-loop stability and process operational safety. Specifically, the constraint of Eq. (23e) forces $W_c(\tilde{x})$ along the predicted state trajectories to decrease at least at the rate under the CLBF-based controller $u = \Phi_{nn}(x) \in U$ when $W_c(x(t_k)) > \rho_{nn}$ and $x(t_k) \notin \mathcal{B}_\delta(x_e)$. If $W_c(x(t_k)) \leq \rho_{nn}$, the constraint of Eq. (23f) is activated to maintain the predicted state of the RNN system within $\mathcal{U}_{\rho_{nn}}$ such that the closed-loop state of the nonlinear system of Eq. (1) is bounded in $\mathcal{U}_{\rho_{\min}}$. Additionally, if $x(t_k) \in \mathcal{B}_\delta(x_e)$, the constraint of Eq. (23g) decreases $W_c(x)$ over the prediction horizon such that the state can escape from saddle points x_e within finite sampling steps. The state measurements of the closed-loop system of Eq. (1) are assumed to be available at each sampling time. After the CLBF-MPC optimization problem of Eq. (23) solves the optimal solution $u^*(t)$, only the first control action of $u^*(t)$ is sent to the control actuators to be applied over the next sampling period. Then, the horizon will be rolled forward one sampling time, and at the next instance of time $t_{k+1} := t_k + \Delta$, the optimization problem is solved again. Additionally, since the CLBF-MPC optimization problem of Eq. (23) is based on the state of the RNN model of Eq. (3) only, we use x instead of $\hat{x}$ to represent the RNN state in CLBF-MPC to simplify the notations.

The theorem below is established to demonstrate that under the CLBF-MPC of Eq. (23), closed-loop stability and process operational safety are achieved simultaneously for the nonlinear system of Eq. (1) in the sense that the closed-loop state is bounded in the safe operating region $\mathcal{U}_\rho$ for all times, and is ultimately bounded in $\mathcal{U}_{\rho_{\min}}$.

Theorem 2. *Consider the system of Eq. (1) with a constrained CLBF W_c that satisfies Eq. (5) and has a minimum at the origin. Given any initial state $x_0 \in \mathcal{U}_\rho$, it is guaranteed that the CLBF-MPC optimization problem of Eq. (23) can be solved with recursive feasibility for all times. Additionally, under the sample-and-hold implementation of CLBF-MPC based on an ensemble of RNN models that satisfy $|\nu| = |F(x,u,0) - F_{nn}(x,u)| \leq \gamma|x| \leq \nu_m$ and the conditions in Proposition 4, it is guaranteed that for any $x_0 \in \mathcal{U}_\rho$, the state is bounded in $\mathcal{U}_\rho$, $\forall\, t \geq 0$, and ultimately converges to $\mathcal{U}_{\rho_{\min}}$ as $t \to \infty$.*

Proof. The proof consists of two parts. The first part presents the proof of recursive feasibility of the CLBF-MPC optimization problem of Eq. (23) for all states $x(t) \in \mathcal{U}_\rho$. The second part includes the proof of simultaneous closed-loop stability and process operational safety of the nonlinear system of Eq. (1) under the CLBF-MPC that uses an ensemble of RNN models of Eq. (3) for prediction.

Part 1: A feasible solution to the CLBF-MPC optimization problem of Eq. (23) exists for all times since it has been demonstrated in Propositions 2–4 that the controllers $u = \Phi_{nn}(x) \in U$, $\forall x \in \mathcal{U}_\rho \backslash \mathcal{B}_\delta(x_e)$ and $u = \bar{u}(x) \in U$, $\forall x \in \mathcal{B}_\delta(x_e)$ in a sample-and-hold fashion satisfy the CLBF-MPC constraints of Eqs. (23d)–(23g). Specifically, the input constraint of Eq. (23d) is satisfied over the prediction horizon since both $u = \Phi_{nn}(x)$ and $u = \bar{u}(x)$ are constrained by $u \in U$. The satisfaction of Eq. (23e) is readily shown by letting $u(t_k) = \Phi_{nn}(x(t_k))$ when $x(t_k) \in \mathcal{U}_\rho \backslash (\mathcal{B}_\delta(x_e) \cup \mathcal{U}_{\rho_{nn}})$. Additionally, the input trajectories $u(t) = \Phi_{nn}(x(t_{k+i})) \in U$, $\forall t \in [t_{k+i}, t_{k+i+1})$ with $i = 0, \ldots, N-1$ is a set of feasible control actions that meet the constraint of Eq. (23f). In Proposition 4, it is shown that once the state is driven into $\mathcal{U}_{\rho_s}$ under the controller $u = \Phi_{nn}(x) \in U$, it will not leave $\mathcal{U}_{\rho_{nn}}$ within one sampling period for any $u \in U$. Therefore, the constraint of Eq. (23f) is satisfied under the sample-and-hold implementation of $u = \Phi_{nn}(x) \in U$. Lastly, if $x(t_k) \in \mathcal{B}_\delta(x_e)$, $u(t) = \bar{u}(x(t_{k+i})) \in U$, $\forall t \in [t_{k+i}, t_{k+i+1})$ with $i = 0, \ldots, N-1$ is a set of control actions that meet the constraint of Eq. (23g) as the controller $u = \bar{u}(x) \in U$ is designed to satisfy Eq. (16) to drive the state away from saddle points. This completes the proof of recursive feasibility for the CLBF-MPC optimization problem of Eq. (23).

Part 2: We first consider the case of an unbounded unsafe region $\mathcal{D}_u$ for the nonlinear system of Eq. (1). As there is no saddle point in the presence of $\mathcal{D}_u$ (i.e., $\mathcal{X}_e = \emptyset$), the last constraint of Eq. (23g) in the CLBF-MPC optimization problem is never activated. Therefore, for any initial condition $x_0 \in \mathcal{U}_\rho \backslash \mathcal{U}_{\rho_{nn}}$, the constraint of Eq. (23e) forces the state to move towards the origin and drives the state into $\mathcal{U}_{\rho_{nn}}$ within finite sampling steps. After the state enters $\mathcal{U}_{\rho_{nn}}$, the constraint of Eq. (23e) ensures the boundedness of the state in $\mathcal{U}_{\rho_{nn}}$ for the remaining time. As a result, the nonlinear system of Eq. (1) is considered practically stable because it has been shown in Proposition 4 that the state of the nonlinear system of Eq. (1) is ultimately bounded in $\mathcal{U}_{\rho_{\min}}$ (a small neighborhood around the origin). Additionally, it should be noted that since the state is also bounded in the safe operating region $\mathcal{U}_\rho$ for all times, which does not intersect with the unbounded unsafe region $\mathcal{D}_u$ in state-space, process operational safety for the system of Eq. (1) is guaranteed under CLBF-MPC.

Following the above analysis, the proof of closed-loop stability and process operational safety for a bounded unsafe region $\mathcal{D}_b$ is presented by showing that the state can be ultimately bounded in $\mathcal{U}_{\rho_{nn}}$ instead of converging to saddle points. Starting from an initial condition $x_0 \in \mathcal{U}_\rho \backslash \mathcal{U}_{\rho_{nn}}$, the constraint of Eq. (23e) drives the state towards the origin. However, the state may settle in saddle points (local minima of the CLBF) along its trajectory towards the origin if no further action is taken around the saddle points. To address this, the constraint of Eq. (23g) is activated when $x(t_k) \in \mathcal{B}_\delta(x_e)$ to move the state away from the saddle points in a direction of decreasing the value of $W_c(x)$ such that the state can escape from saddle points and ultimately converge to the origin. Once the state leaves the neighborhood $\mathcal{B}_\delta(x_e)$ around the saddle points, closed-loop stability and process operation safety are still guaranteed under the constraints of Eqs. (23e)–(23f) in the sense that the state of the nonlinear system of Eq. (1) stays in the safe operating region $\mathcal{U}_\rho$ for all times, and is ultimately maintained in $\mathcal{U}_{\rho_{nn}}$. This completes the proof of simultaneous closed-loop stability and process operation safety for both an unbounded unsafe region and a bounded unsafe region. □

Remark 3. The training dataset for the RNN models used in MPC is generated from extensive open-loop simulations using various control actions $u \in U$ and different initial conditions x_0 in the operation region. To ensure that the RNN models are sufficiently accurate for the controller design, the training process of RNN models is terminated only if the modeling error is rendered below a predetermined threshold (i.e., the modeling error is sufficiently small). Therefore, the modeling error constraint guarantees that the obtained RNN models can well represent the nonlinear dynamics in the operating region, and is also a sufficient condition for the proof of closed-loop stability and safety for the MPC using RNN models.

4. Application to a chemical process example

In this section, a chemical process example is utilized to illustrate the application of the proposed CLBF-MPC scheme that incorporates an ensemble of RNN models for prediction. We consider a well-mixed, non-isothermal continuous stirred tank reactor (CSTR) where an irreversible second-order exothermic reaction takes place. The reaction converts the reactant A to the product B via the chemical reaction $A \to B$. A heating jacket that supplies or removes heat from the reactor is used. The CSTR dynamic model

Table 1
Parameter values of the CSTR.

$T_0 = 300\ K$	$F = 5\ m^3/hr$
$V = 1\ m^3$	$E = 5 \times 10^4\ kJ/kmol$
$k_0 = 8.46 \times 10^6\ m^3/kmol\ hr$	$\Delta H = -1.15 \times 10^4\ kJ/kmol$
$C_p = 0.231\ kJ/kg\ K$	$R = 8.314\ kJ/kmol\ K$
$\rho_L = 1000\ kg/m^3$	$C_{A0_s} = 4\ kmol/m^3$
$Q_s = 0.0\ kJ/hr$	

derived from material and energy balances is given below:

$$\frac{dC_A}{dt} = \frac{F}{V}(C_{A0} - C_A) - k_0 e^{\frac{-E}{RT}} C_A^2 \tag{24a}$$

$$\frac{dT}{dt} = \frac{F}{V}(T_0 - T) + \frac{-\Delta H}{\rho_L C_p} k_0 e^{\frac{-E}{RT}} C_A^2 + \frac{Q}{\rho_L C_p V} \tag{24b}$$

where C_A is the concentration of reactant A in the reactor, V is the volume of the reacting liquid in the reactor, T is the temperature of the reactor and Q denotes the heat input rate. The concentration of reactant A in the feed is C_{A0}. The feed temperature and volumetric flow rate are T_0 and F, respectively. The reacting liquid has a constant density of ρ_L and a heat capacity of C_p. ΔH, k_0, E, and R represent the enthalpy of reaction, pre-exponential constant, activation energy, and ideal gas constant, respectively. Process parameter values are listed in Table 1.

The CSTR is initially operated at the unstable steady-state $(C_{As},\ T_s) = (1.95\ kmol/m^3,\ 402\ K)$, and $(C_{A0_s}\ Q_s) = (4\ kmol/m^3,\ 0\ kJ/hr)$. The manipulated inputs are the inlet concentration of species A and the heat input rate, which are represented by the deviation variables $\Delta C_{A0} = C_{A0} - C_{A0_s}$, and $\Delta Q = Q - Q_s$, respectively. The manipulated inputs are bounded as follows: $|\Delta C_{A0}| \leq 3.5\, kmol/m^3$ and $|\Delta Q| \leq 5 \times 10^5\, kJ/hr$. The states and the inputs of the closed-loop system are $x^T = [C_A - C_{As}\ T - T_s]$ and $u^T = [\Delta C_{A0}\ \Delta Q]$, respectively, such that the equilibrium point of the system is at the origin of the state-space, (i.e., $(x_s^*, u_s^*) = (0, 0)$).

The explicit Euler method with an integration time step of $h_c = 2 \times 10^{-5}\ hr$ is applied to numerically simulate the dynamic model of Eq. (24). The nonlinear optimization problem of the CLBF-MPC of Eq. (23) is solved using the python module of the IPOPT software package (Wächter and Biegler, 2006), named PyIpopt with the sampling period $\Delta = 2 \times 10^{-3}\ hr$.

4.1. Development of RNN models

To develop an ensemble of RNN models that will be used in CLBF-MPC, extensive open-loop simulations are performed within the operating region for the CSTR of Eq. (24) to generate the dataset. Specifically, we run open-loop simulations with various initial states in state-space and inputs $u \in U$ for finite sampling steps such that the dataset is sufficiently large to be representative in the operating region. The sampled data points including states x and inputs u are saved with a minimum time step as the integration time step h_c. The RNN model is constructed with one input layer, two hidden layers consisting of 96 and 64 recurrent units, respectively, and one output layer. The inputs to the RNN model of Eq. (3) are the states $x(t_k)$ and the control actions $u(t_k)$ at $t = t_k,\ k = 0, 1, \ldots,$ and the outputs are the predicted state trajectory over one sampling period (i.e., $t \in [t_k, t_{k+1}]$), where the data points with the time interval of h_c (i.e., the integration time step for the explicit Euler method) are treated as the internal states for RNN models. The sigmoid function is used as the activation function for RNN models, and early stopping is employed to avoid overfitting. Additionally, we utilize a 10-fold cross validation to derive an ensemble of 10 RNN models for the CLBF-MPC of Eq. (23). The optimal number of recurrent neural network models in the ensemble generally depends on the complexity of process dynamics and the size of datasets. In our CSTR example, the optimal number is determined by closed-loop simulations. Specifically, to determine the optimal number of neural network models, we first derive k RNN models based on a k-fold cross-validation. Subsequently, we start with a single RNN model and keep increasing the number of models used in MPC. The optimal number is determined to be the one when no further improvement of closed-loop performance is noticed for the increase of RNN models being used. The details of developing RNN models for this CSTR example can be found in Wu et al. (2019c).

4.2. Simulation results

The control objective is to operate the CSTR at the unstable equilibrium point (C_{As}, T_s) and avoid the unsafe operating region (bounded and unbounded) in state-space by manipulating the heat input rate ΔQ and the inlet concentration ΔC_{A0} under the RNN-based CLBF-MPC.

We first demonstrate the application of the proposed CLBF-MPC control scheme to an unbounded unsafe region $\mathcal{D}_u$ in state-space. The unsafe region is characterized as an unbounded set with high temperature and concentration for the CSTR of Eq. (24): $\mathcal{D}_u := \{x \in \mathbf{R}^2 \mid F(x) = x_1 + x_2 > 47\}$. It is noted that with the form of $F(x) = x_1 + x_2$, the temperature in the reactor is considered the dominant factor in characterizing the unsafe region $\mathcal{D}_u$, while the reactant concentration is also accounted for because of its impact on the reaction rate $r = k_0 e^{-E/RT} C_A^2$. Following the construction method of a CLBF in Wu et al. (2018, 2019a), we first design a Control Lyapunov function with the standard quadratic form $V(x) = x^T P x$, where P is a positive definite matrix as follows:

$$P = \begin{bmatrix} 1060 & 22 \\ 22 & 0.52 \end{bmatrix} \tag{25}$$

Then, we characterize a set $\mathcal{H}$ that contains $\mathcal{D}_u$: $\mathcal{H} := \{x \in \mathbf{R}^2 \mid F(x) > 45\}$, and design the Control Barrier function $B(x)$ as follows:

$$B(x) = \begin{cases} e^{F(x)-47} - 2 \times e^{-2}, & \text{if } x \in \mathcal{H} \\ -e^{-2}, & \text{if } x \notin \mathcal{H} \end{cases} \tag{26}$$

The Control Lyapunov-Barrier function $W_c(x) = V(x) + \mu B(x) + \nu$ is constructed with the following parameters: $\rho = 0$, $c_1 = 0.1$, $c_2 = 1061$, $c_3 = 5808$, $c_4 = 2259$, $\nu = \rho - c_1 c_4 = -225.9$, and $\mu = 4.6 \times 10^7$. The definitions of the above parameters can be found in Wu et al. (2018, 2019a). It is demonstrated in Fig. 1 that under the CLBF-MPC of Eq. (23), all the trajectories starting from initial states in $\mathcal{U}_{\hat{\rho}}$ (a subset of the safe operating region $\mathcal{U}_\rho$ in state-space) avoid the unbounded unsafe region $\mathcal{D}_u$ on the top and converge to $\mathcal{U}_{\rho_{\min}}$.

The second example is used to demonstrate that the state of the closed-loop system of Eq. (24) can avoid a bounded unsafe region $\mathcal{D}_b$ in state-space under the CLBF-MPC of Eq. (23) and converge to a small neighborhood around the origin. To demonstrate that the state is able to pass around the unsafe region along the trajectory towards the origin, we design a bounded unsafe region $\mathcal{D}_b$ embedded within the safe operating region as shown in the above example. Specifically, the unsafe region is defined as an ellipse: $\mathcal{D}_b := \{x \in \mathbf{R}^2 \mid F(x) = \frac{(x_1+0.92)^2}{1} + \frac{(x_2-42)^2}{500} < 0.06\}$. $\mathcal{H}$ is defined as $\mathcal{H} := \{x \in \mathbf{R}^2 \mid F(x) < 0.07\}$. The Control Barrier function $B(x)$ is defined as follows:

$$B(x) = \begin{cases} e^{\frac{F(x)}{F(x)-0.07}} - e^{-6}, & \text{if } x \in \mathcal{H} \\ -e^{-6}, & \text{if } x \notin \mathcal{H} \end{cases} \tag{27}$$

Using the same Control Lyapunov function $V(x)$ as in the first example, the Control Lyapunov-Barrier function $W_c(x) = V(x) +$

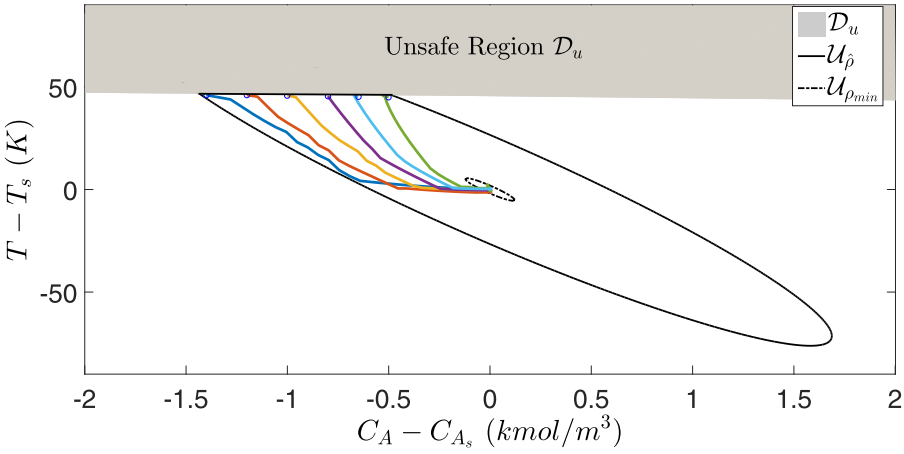

Fig. 1. Closed-loop state trajectories for the system of Eq. (24) under the CLBF-MPC using an ensemble of RNN models. The initial conditions are marked by circles, and the set of unbounded unsafe states $\mathcal{D}_u$ is the gray area on the top.

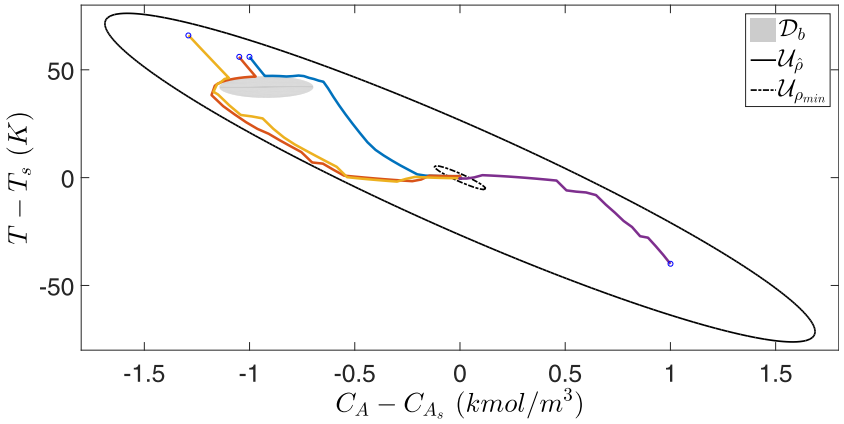

Fig. 2. Closed-loop state trajectories for the system of Eq. (24) under the CLBF-MPC using an ensemble of RNN models. The initial conditions are marked by circles, and the set of bounded unsafe states $\mathcal{D}_b$ is the gray area embedded within $\mathcal{U}_{\hat{\rho}}$.

$\mu B(x) + \nu$ is constructed following the rules in Proposition 1 in Wu et al. (2018), where the values of parameters c_1, c_2, c_3, c_4, ν, and μ can be found in Wu et al. (2018). Additionally, we calculate the stationary point of $W_c(x)$ (other than the origin) in state-space by letting $\frac{\partial W_c(x)}{\partial x} = 0$. It is obtained that the stationary point is $x_e = (-1.004,\ 47.48)$ and it turns out to be a saddle point from a second partial derivative test (i.e., x_e is a saddle point if the determinant of the Hessian matrix of $W_c(x)$ at x_e is negative).

In Fig. 2, it is demonstrated that for all initial states x_0 in $\mathcal{U}_{\hat{\rho}}$ (marked by circles), the closed-loop trajectories avoid the bounded unsafe region $\mathcal{D}_b$ that is embedded within $\mathcal{U}_{\hat{\rho}}$ (a subset of the safe operating region $\mathcal{U}_\rho$), and ultimately converges to $\mathcal{U}_{\rho_{\min}}$ under the CLBF-MPC of Eq. (23). Additionally, to demonstrate the merits of the machine-learning-based CLBF-MPC in terms of desired prediction accuracy and guaranteed process operational safety, a linear state-space model is derived using the same dataset for the RNN models to approximate the nonlinear dynamics in the operating region for comparison. Specifically, the linear state-space model for the CSTR system of Eq. (24) is developed with the following form:

$$\dot{x} = A_s x + B_s u \tag{28}$$

where x and u are the state vector and the manipulated input vector, and A_s and B_s are coefficient matrices for the state-space model. Following the system identification method in Kheradmandi and Mhaskar (2018), the numerical algorithms for subspace state space system identification is utilized to obtain A_s and B_s as follows:

$$A_s = 100 \times \begin{bmatrix} -0.154 & -0.003 \\ 5.19 & 0.138 \end{bmatrix} \tag{29}$$

$$B_s = \begin{bmatrix} 4.03 & 0 \\ 1.23 & 0.004 \end{bmatrix} \tag{30}$$

It is shown in Fig. 3 that for some initial conditions in $\mathcal{U}_{\hat{\rho}}$, the closed-loop state trajectories are able to avoid the unsafe region and converge to the steady-state under the MPC using a linear model. However, in Fig. 4, it is demonstrated that for some other initial conditions, the state trajectories (with dashed line) enter the unsafe region due to a considerable model mismatch of the linear state-space model. It is noted that the model predictive controller using a simple linear state-space model is generally able to stabilize the nonlinear system in a neighborhood around the steady-state provided that the model mismatch between the linear model and the nonlinear system is small in the neighborhood. However, the MPC using a linear state-space model does not work in this example because in addition to closed-loop stability, we are addressing process operational safety that requires a sufficiently small model mismatch for which feedback control without an accurate process model cannot guarantee that the process state avoids the unsafe region for all times. In fact, in the presence of a large model mismatch, feedback control cannot prevent the state from entering the unsafe region since the state predicted by the

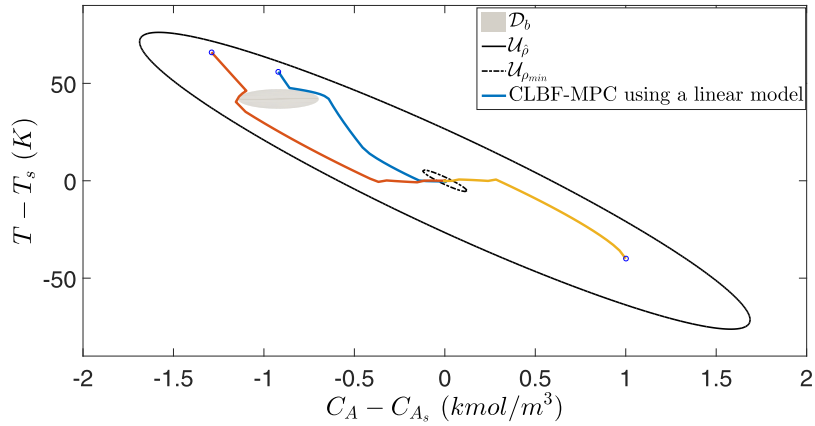

Fig. 3. Closed-loop state trajectories for the CSTR system under the CLBF-MPC using a linear state-space model. The initial conditions are marked by circles, and the set of bounded unsafe states $\mathcal{D}_b$ is the gray ellipse in state-space.

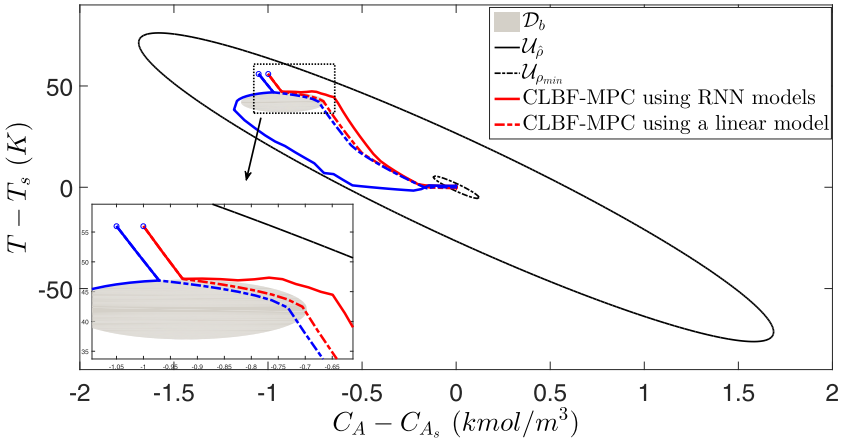

Fig. 4. Comparison of the closed-loop state trajectories under the CLBF-MPC using a linear state-space model (dashed lines) and an ensemble of RNN models (solid lines), respectively. The initial conditions are marked by circles, and the set of bounded unsafe states $\mathcal{D}_b$ is the gray ellipse in state-space.

linear model may be outside of the unsafe region while the true state actually enters it within one sampling period. Therefore, it motivates us to use an ensemble of RNN models with a sufficiently small model mismatch to approximate nonlinear dynamics in the operating region and provide sufficiently accurate predictions for MPC.

The above two case studies demonstrate that the RNN models that are developed from extensive open-loop simulations to replace the CSTR process of Eq. (24) in CLBF-MPC achieve a desired approximation performance. Subsequently, the CLBF-MPC of Eq. (23) based on an ensemble of RNN models guarantees that for any initial condition in the safe operating region, the state of the closed-loop system of Eq. (24) is maintained within the safe operating region for all times, and is able to converge to a small neighborhood $\mathcal{U}_{\rho_{\min}}$ around the origin ultimately while avoiding the unsafe region (bounded and unbounded) in state-space.

5. Conclusion

In this work, a CLBF-MPC method formulated with machine learning models was developed for nonlinear process systems. Under the assumption that the modeling error between the RNN model and the nonlinear process is sufficiently small, sufficient conditions such that simultaneous closed-loop stability and process operational safety in the sense of boundedness of the closed-loop state in the safe operating region, convergence to the origin, and avoidance of the unsafe region are guaranteed for the nonlinear process under the RNN-based CLBF-MPC were derived. Specifically, it was demonstrated that in the presence of a bounded unsafe region, discontinuous control actions were applied in a neighborhood around the saddle point to help the state escape from saddle points and move towards the origin. A chemical process example demonstrated the application of the proposed method to both bounded and unbounded unsafe regions. From the simulation results, it was demonstrated that the RNN-based CLBF-MPC achieved desired prediction results, and thus, the state was successfully driven to the origin while avoiding the unsafe region in state-space.

Declaration of Competing Interest

The authors declare that they have no known competing financial interests or personal relationships that could have appeared to influence the work reported in this paper.

CRediT authorship contribution statement

Zhe Wu: Conceptualization, Methodology, Software, Writing - original draft. **Panagiotis D. Christofides:** Supervision, Writing - review & editing.

Acknowledgments

Financial support from the National Science Foundation and the Department of Energy is gratefully acknowledged.

Supplementary material

Supplementary material associated with this article can be found, in the online version, at doi:10.1016/j.compchemeng.2019.106706.

References

Ali, J.M., Hussain, M.A., Tade, M.O., Zhang, J., 2015. Artificial intelligence techniques applied as estimator in chemical process systems–a literature survey. Expert Syst. Appl. 42, 5915–5931.

Ames, A.D., Grizzle, J.W., Tabuada, P., 2014. Control barrier function based quadratic programs with application to adaptive cruise control. In: Proceedings of the 53rd IEEE conference on decision and control, pp. 6271–6278. Los Angeles, California

Ames, A.D., Xu, X., Grizzle, J.W., Tabuada, P., 2016. Control barrier function based quadratic programs for safety critical systems. IEEE Trans. Autom. Control 62, 3861–3876.

Billings, S.A., 2013. Nonlinear System Identification: NARMAX Methods in the Time, Frequency, and Spatio-Temporal Domains. John Wiley & Sons.

Braun, P., & Kellett, C. M. (2018). On (the existence of) control Lyapunov barrier functions. Preprint, https://www.eref.uni-bayreuth.de/40899.

Incidents, C. I. o. C. (2016). Final Report of the Investiagtions of Chemical Incidents. Technical Report, U.S. Chemical Safety and Hazard Investigation Board.

Jankovic, M., 2017. Combining control Lyapunov and barrier functions for constrained stabilization of nonlinear systems. In: Proceedings of the american control conference, pp. 1916–1922. Seattle, Washington

Kheradmandi, M., Mhaskar, P., 2018. Data driven economic model predictive control. Mathematics 6, 51.

Kosmatopoulos, E.B., Polycarpou, M.M., Christodoulou, M.A., Ioannou, P.A., 1995. High-order neural network structures for identification of dynamical systems. IEEE Trans. Neural Netw. 6, 422–431.

Lin, Y., Sontag, E.D., 1991. A universal formula for stabilization with bounded controls. Syst. Control Lett. 16, 393–397.

Malisoff, M., Mazenc, F., 2009. Constructions of Strict Lyapunov Functions. Springer Science & Business Media.

Mendes-Moreira, J., Soares, C., Jorge, A.M., Sousa, J.F.D., 2012. Ensemble approaches for regression: a survey. ACM Comput. Surv. 45, 10.

Niu, B., Zhao, J., 2013. Barrier Lyapunov functions for the output tracking control of constrained nonlinear switched systems. Syst. Control Lett. 62, 963–971.

Romdlony, M.Z., Jayawardhana, B., 2016. Stabilization with guaranteed safety using control Lyapunov–barrier function. Automatica 66, 39–47.

Sanders, R.E., 2015. Chemical Process Safety: Learning From Case Histories. Butterworth-Heinemann.

Sontag, E.D., 1989. A 'universal' construction of Artstein's theorem on nonlinear stabilization. Syst. Control Lett. 13, 117–123.

Tee, K.P., Ge, S.S., Tay, E.H., 2009. Barrier Lyapunov functions for the control of output-constrained nonlinear systems. Automatica 45, 918–927.

Trischler, A.P., D'Eleuterio, G.M., 2016. Synthesis of recurrent neural networks for dynamical system simulation. Neural Netw. 80, 67–78.

Van Overschee, P., De Moor, B., 1994. N4SID: Subspace algorithms for the identification of combined deterministic-stochastic systems. Automatica 30, 75–93.

Viberg, M., 1995. Subspace-based methods for the identification of linear time-invariant systems. Automatica 31, 1835–1851.

Wächter, A., Biegler, L.T., 2006. On the implementation of an interior-point filter line-search algorithm for large-scale nonlinear programming. Math. Program. 106, 25–57.

Wieland, P., Allgöwer, F., 2007. Constructive safety using control barrier functions. IFAC Proc. Vol. 40, 462–467.

Wong, W., Chee, E., Li, J., Wang, X., 2018. Recurrent neural network-based model predictive control for continuous pharmaceutical manufacturing. Mathematics 6, 242.

Wu, Z., Albalawi, F., Zhang, Z., Zhang, J., Durand, H., Christofides, P.D., 2019a. Control Lyapunov-barrier function-based model predictive control of nonlinear systems. Automatica 109, 108508.

Wu, Z., Christofides, P.D., 2019. Handling bounded and unbounded unsafe sets in control Lyapunov-barrier function-based model predictive control of nonlinear processes. Chem. Eng. Res. Des. 143, 140–149.

Wu, Z., Durand, H., Christofides, P.D., 2018. Safe economic model predictive control of nonlinear systems. Syst. Control Lett. 118, 69–76.

Wu, Z., Tran, A., Rincon, D., Christofides, P.D., 2019b. Machine learning-based predictive control of nonlinear processes. Part I: theory. AIChE J. 65, e16729.

Wu, Z., Tran, A., Rincon, D., Christofides, P.D., 2019c. Machine learning-based predictive control of nonlinear processes. Part II: computational implementation. AIChE J. 65, e16734.

Zhang, C., Ma, Y., 2012. Ensemble Machine Learning: Methods and Applications. Springer.